Acta Crystallographica Section D
Biological Crystallography
ISSN 0907-4449

A systematic study of 50S ribosomal subunit purification enabling robust crystallization

Thomas J. McLellan,[a] Eric S. Marr,[a] Lillian M. Wondrack,[b] Timothy A. Subashi,[a] Paul A. Aeed,[a]‡ Seungil Han,[a] Zuoyu Xu,[b]§ Ing-Kae Wang[a]¶ and Bruce A. Maguire[a]*

[a]Pfizer Inc., Department of Exploratory Medicinal Sciences, Pfizer Global Research and Development, Eastern Point Road, Groton, CT 06340, USA, and [b]Pfizer Inc., Department of Antibacterials, Pfizer Global Research and Development, Eastern Point Road, Groton, CT 06340, USA

‡ Present address: Pfizer Animal Health, Veterinary Medicine Research and Development, 333 Portage Street, Kalamazoo, MI 49007, USA.
§ Present address: Bacteriology and Mycology Branch, National Institute of Allergy and Infectious Diseases, National Institutes of Health, 6610 Rockledge Drive, Bethesda, MD 20892-6603, USA.
¶ Present address: Novartis Institutes for BioMedical Research Inc., 200 Technology Square, Cambridge, MA 02139, USA.

Correspondence e-mail: bruce.maguire@pfizer.com

Received 2 June 2009
Accepted 25 September 2009

A systematic analysis was undertaken to seek correlations between the integrity, purity and activity of 50S ribosomal subunit preparations from *Deinococcus radiodurans* and their ability to crystallize. Conditions of fermentation, purification and crystallization were varied in a search for crystals that could reliably supply an industrial X-ray crystallography program for the structure-based design of ribosomal antibiotics. A robust protocol was obtained to routinely obtain crystals that gave diffraction patterns extending to 2.9 Å resolution and that were large enough to yield a complete data set from a single crystal. To our knowledge, this is the most systematic study of this challenging area so far undertaken. Ribosome crystallization is a complex multi-factorial problem and although a clear correlation of crystallization with subunit properties was not obtained, the search for key factors that potentiate crystallization has been greatly narrowed and promising areas for further inquiry are suggested.

1. Introduction

Diffracting crystals of ribosomes for structure determination were first obtained nearly 30 years ago (Yonath *et al.*, 1980), yet the essential parameters that govern which ribosome preparations will crystallize remain obscure. The bacterial ribosome (denoted '70S' according to its sedimentation coefficient) is comprised of one small ('30S') ribosomal subunit and one large ('50S') ribosomal subunit, for which high-resolution crystallographic structures were obtained in 2001 (Harms *et al.*, 2001; Schluenzen *et al.*, 2000; Wimberly *et al.*, 2000). We set out to obtain diffracting crystals of the 50S ribosomal subunit, which is the target of marketed antibiotics such as Zithromax and Zyvox, as part of a structure-based drug-design program aimed at developing new or improved antibiotics. To be useful in an industrial setting, structures with bound drug candidates must be routinely generated to inform iterative cycles of design, synthesis and testing of drug candidates. This dictates that the generation of crystals must be robust and reliable in order to avoid costly delays.

The 50S subunits from the halophilic archaeon *Haloarcula marismortui* crystallize readily and routinely diffract to below 3 Å resolution (von Bohlen *et al.*, 1991). Although we were able to obtain such crystals, we chose instead to focus our efforts on the 50S subunit of the radiation- and desiccation-resistant eubacterium *Deinococcus radiodurans* because, like most pathogens. it is a eubacterium (Gluehmann *et al.*, 2001; Harms *et al.*, 2001), while *H. marismortui* is an archaeon and so has ribosomes that are more similar to eukaryotic ribosomes than eubacterial ones are (Hartman *et al.*, 2006). Small but significant differences in the way that antibiotics bind to the 50S subunit from the archaeal and eubacterial domains have

been reported (Wilson *et al.*, 2005; Yonath, 2002). Furthermore, halophilic ribosomes, such as those from *H. marismortui*, require high salt concentrations to maintain their integrity; this can limit the solubility of drug candidates that are soaked into the crystals to determine cocrystal structures. Finally, although *D. radiodurans* is an extremophile that is adapted to survive radiation and desiccation, unlike *H. marismortui*, which requires high salinity, or *Thermus thermophilus*, which requires high temperature, it does not require extreme conditions for growth. Similarly, ribosomes from *H. marismortui* or *T. thermophilus* are adapted to function at high salinity or temperature, respectively, while those from *D. radiodurans* do not require extreme conditions for optimal activity and so may serve as a better model system to understand how to obtain crystals from more clinically relevant non-extremophile organisms in the future. However, it is possible that small molecules or ions may help to protect its ribosomes from damage (Suessmuth & Widmann, 1979). If such extrinsic factors were found to assist in the purification of crystallizable subunits, they could then be applied to ribosomes of other species. The extra difficulty of working with the *D. radiodurans* 50S subunit was thus offset by the potential long-term benefits.

In order to crystallize, ribosomes must be highly pure and active (Yonath *et al.*, 1982), yet this does not guarantee success. For ribosomes from an organism such as *D. radiodurans*, even a tried and tested purification method may have to be repeated two or three times to yield subunits that crystallize. This low rate of success is a considerable handicap to improving crystallization, as the element of randomness necessitates multiple evaluations of each new parameter. On the other hand, if the source of this variability could be understood and controlled, the crystallization of subunits from other organisms might then become possible. We therefore set out first to obtain 50S subunits of *D. radiodurans* that crystallize, and then to improve the reliability of the subunits so that every preparation crystallizes. This enabled further systematic improvement in preparations so that larger better diffracting crystals could be obtained efficiently enough to drive a robust industrial structure-based drug-design program.

2. Materials and methods

2.1. Reagents

Yeast extract was from Difco (catalog No. 212750). Tryptone was from Oxoid Ltd (catalog No. LP0042) unless otherwise stated. All other chemicals were from JT Baker.

2.2. Growth of *D. radiodurans*

D. radiodurans strain DSMZ 20539 was grown in an IF-150 fermentor (New Brunswick Scientific Co. Inc.) at 303 K with 400 rev min^{-1} agitation and 20 l min^{-1} aeration. 2 l of actively growing overnight culture was used to inoculate 38 l of growth medium to an A_{600} of 0.15. Cultures grew with a doubling time of about 100 min. At an A_{600} of 3, the culture was cooled to 288 K over 15 min and about 180 g cell paste was harvested by refrigerated continuous-flow centrifugation (Contifuge, Heraeus Inc.) and stored at 193 K. The growth medium was 10 g tryptone, 5 g glucose, 5 g yeast extract, 5 g NaCl per litre at pH 7.2 supplemented with manganese sulfate monohydrate (0.82 mg l^{-1}). Some early experiments used tryptone from Difco Inc. (catalog No. 211705) or casein hydrolysate (Oxoid Ltd; catalog No. LP0041).

2.3. Purification of 50S subunits from *D. radiodurans*

2.3.1. Isolation from polysomes. Subunits were isolated as previously described (Auerbach-Nevo *et al.*, 2005) but without a dialysis step.

2.3.2. Isolation from loose- and tight-couple ribosomes. All procedures were conducted at 277 K. 40 g of cell paste was thawed and resuspended in 80 ml lysis buffer (10 m*M* HEPES–NaOH pH 7.8, 30 m*M* $MgCl_2$, 150 m*M* NH_4Cl, 6 m*M* β-mercaptoethanol). Cells were broken by passage through a French pressure cell at 69 MPa. RNase-free DNase was added (Roche Diagnostics Corp.) and the lysate was incubated on ice for 30 min. Unbroken cells were spun down for 30 min at 18.5 krev min^{-1} in a Sorvall SS-34 rotor. The supernatant was removed and 0.2 volumes of 1.1 *M* sucrose solution in lysis buffer were added to it before centrifugation for 2 h at 19 krev min^{-1} in a Beckman Type 50.2 Ti rotor to pellet the polysomes and membrane fragments. The supernatant was transferred to fresh tubes and underlaid with 5 ml of the 1.1 *M* sucrose solution and centrifuged at 40 krev min^{-1} for 17–19 h in the same rotor to pellet the ribosomes. The supernatant was discarded and the pellets were resuspended in 1 ml lysis buffer per tube on a wrist-action shaker (Burrell Inc.). The resuspended ribosomes were then dialyzed in 10 kDa molecular-weight cutoff dialysis tubing twice against 1 l lysis buffer for 3 h and clarified by centrifugation at 15 krev min^{-1} for 10 min in a Sorvall SS-34 rotor. The supernatant was loaded onto a 10–40%(*w*/*v*) linear sucrose density gradient in 6 m*M* magnesium buffer (10 m*M* HEPES–NaOH pH 7.8, 6 m*M* $MgCl_2$, 100 m*M* NH_4Cl, 6 m*M* β-mercaptoethanol) and centrifuged at 27 krev min^{-1} for 17.5 h in a Beckman Ti-15 zonal rotor. The gradient was fractionated using an ISCO Type 11 optical cell and model UA6 absorbance monitor. Fractions containing 50S subunits (the mixed free and loose-couple-derived 50S) or the 70S ribosomes were separately pooled and the magnesium concentration was raised to 10 m*M* by the gradual addition, with stirring, of 1/3 volume of gradient buffer supplemented with additional $MgCl_2$ to 17.3 m*M*; they were then centrifuged at 40 krev min^{-1} for 19 h in a Beckman Type 45 rotor. Pellets of 50S subunits were resuspended on a wrist-action shaker in resuspension buffer (10 m*M* HEPES–NaOH pH 7.8, 15 m*M* $MgCl_2$, 75 m*M* NH_4Cl, 6 m*M* β–mercaptoethanol). Pellets of 70S subunits were resuspended in a total of 10 ml lysis buffer diluted to 50 ml in 1 m*M* magnesium buffer (10 m*M* HEPES–NaOH pH 7.8, 1 m*M* $MgCl_2$, 100 m*M* NH_4Cl, 6 m*M* β-mercaptoethanol) and loaded onto a 10–40%(*w*/*v*) linear sucrose density gradient made in the same buffer. Centrifugation was at 28 krev min^{-1} for 19 h in a Beckman Ti-15 zonal rotor. Fractions containing 50S were pooled and the magnesium

concentration was raised to 10 m*M* by the addition of 1/3 volume of buffer supplemented with magnesium to 39 m*M*. The 50S subunits were pelleted and resuspended as for the free/loose 50S. Finally, the two 50S samples were repelleted in a Beckman TLA100.2 rotor at 80 krev min^{-1} for 1 h and resuspended to a final concentration of 800–1000 A_{260} ml^{-1} in resuspension buffer. The resuspended samples were microfuged at full speed for 15 min to remove any particulates and the supernatant was aliquotted and then flash-frozen in liquid nitrogen for storage at 193 K.

2.3.3. 'Direct' isolation. All procedures were conducted at 277 K. Lysates were prepared and unbroken cells were removed as in §2.3.2. The lysate was then directly loaded onto a 10–40%(*w*/*v*) linear sucrose density gradient in lysis buffer and centrifuged at 27 krev min^{-1} for 16.5 h in a Beckman Ti-15 zonal rotor. Lysis buffer was used for this first gradient rather than a buffer with lower magnesium-ion concentration since the goal here was to isolate 70S ribosomes rather than their dissociation products. The gradient was pumped out through an ISCO UA-5 absorbance monitor and fractions containing 70S ribosomes were pooled and pelleted by centrifugation at 40 krev min^{-1} for 19 h in a Beckman Type 45 rotor. In later experiments this pelleting step was replaced by concentration of the 70S ribosomes in an Amicon stirred cell (Millipore Inc.) using a 76 mm diameter YM-100 membrane under nitrogen pressure with several changes of lysis buffer to reduce the sucrose concentration to 8% (as judged by refractive index) in a final volume of 25 ml. This was diluted 1:1 with 1 m*M* magnesium gradient buffer and loaded onto a 10–40%(*w*/*v*) linear sucrose density gradient in 1 m*M* magnesium buffer and centrifuged at 28 krev min^{-1} for 19 h in a Beckman Ti-15 zonal rotor. Fractions containing the 50S subunits were pooled and the magnesium concentration was raised to 10 m*M* as before by the addition of 1/3 volume of buffer supplemented with magnesium to 39 m*M*. The 50S subunits were then either pelleted as in §2.3.2 and resuspended in resuspension buffer or subjected to ultrafiltration and buffer exchange to reduce the sucrose concentration to 2% or lower before pelleting in a Beckman Type 65 rotor (50 krev min^{-1} for 2.5 h) and resuspension in resuspension buffer. Samples were clarified, aliquotted, frozen and stored as for the loose/tight-couple-derived subunits.

2.3.4. Purification variants. For more rapid 70S isolation, the sucrose concentrations in the first gradient could be halved to 5–20%(*w*/*v*) and the gradient centrifuged at 32 krev min^{-1} for only 5.5 h. To test the effect of protease inhibitors, duplicate samples were processed in parallel but for one the lysis buffer was supplemented with protease inhibitors (one tablet of Roche Complete plus EDTA per 50 ml) and 0.1 m*M* EDTA and 0.1 m*M* extra $MgCl_2$ were added to the sucrose gradient buffer. To test the effect of EDTA alone, the lysis buffer was supplemented with an extra 1 m*M* $MgCl_2$ and 1 m*M* EDTA, and 0.1 m*M* EDTA and 0.1 m*M* extra $MgCl_2$ were added to the sucrose gradient buffer.

To polish purified subunits by pelleting through a sucrose cushion, 100 A_{260} units of purified 50S were diluted in 8 ml resuspension buffer, underlaid with 2 ml 1.1 *M* sucrose in the same buffer and centrifuged at 45 krev min^{-1} in a Beckman Type 65 rotor for 17 h. The pellet was resuspended in 1 ml resuspension buffer, repelleted at 60 krev min^{-1} for 1.75 h in a Beckman TLA 100.2 rotor, resuspended in resuspension buffer and clarified by microfuging for 15 min.

To polish purified subunits by chromatography on cysteine-Sulfolink resin, 300 A_{260} units of purified 50S were loaded onto a 20 ml column of resin equilibrated in resuspension buffer, washed with five column volumes and then eluted with a gradient of resuspension buffer to lysis buffer supplemented with 500 m*M* NH_4Cl over ten column volumes. Fractions containing the subunits were pooled, diluted twofold with resuspension buffer, concentrated by ultrafiltration and pelleted by centrifugation at 28 krev min^{-1} for 15 h in a Beckman Type 65 rotor. Pellets were resuspended in resuspension buffer and clarified by microfuging for 15 min.

To purify ribosomes by chromatography on cysteine-Sulfolink resin prior to isolation of 50S by centrifugation as in §2.3.3, a lysate was prepared as in §2.3.2 and filtered through a 0.22 µm filter (GP Express plus Stericup; Millipore Inc.) before loading onto a 125 ml column of resin at 0.5 ml min^{-1} on an ÄKTA chromatography platform (GE Healthcare). The column was washed with ten column volumes of lysis buffer and then eluted with a gradient over ten column volumes to 100% lysis buffer supplemented with 500 m*M* NH_4Cl. Fractions were pooled, concentrated in an Amicon stirred cell and the buffer was exchanged for lysis buffer to give a final sample in 20 ml lysis buffer for loading onto a gradient in lysis buffer to begin the direct isolation protocol.

2.4. General analytical methods

Proteins and rRNA were extracted, electrophoresed and visualized as previously described (Maguire *et al.*, 2008). Analytical sucrose density-gradient centrifugation was also performed as previously described (Maguire *et al.*, 2008). PolyU-directed translation was carried out as previously described (Auerbach-Nevo *et al.*, 2005) using a twofold excess of 30S subunits over 50S subunits.

2.5. Extraction of proteins for LC-MS

120 µg 50S subunits (2.5 A_{260} units) was diluted to a volume of 6.25 µl in resuspension buffer. 20 µl 10.5 *M* urea containing 1% β-mercaptoethanol was added, followed by 0.1 volume of 1 *M* $MgCl_2$ and two volumes of acetic acid. Samples were incubated on ice for 45 min with occasional mixing and then microfuged for 15 min at 277 K to pellet the RNA. The supernatant (containing about 1 pmol of 50S proteins per microlitre) was removed and stored at 253 K for MS analysis. Prior to injection on the LC-MS, bovine ribonuclease A was added (to 1 pmol µl^{-1} final concentration) as an internal standard for normalization to obtain relative quantitation between preparations.

2.6. Identification of ribosomal proteins extracted from 50S subunits

LC-MS and fraction collection were performed using an Agilent 1100 binary HPLC system with a diode-array absorbance detector. For the protein-identification experiments, the

effluent was split to a Micromass LCT ESI–TOF mass spectrometer and a Pharmacia Frac100 fraction collector. The electrospray interface of the mass spectrometer was operated in the positive-ion mode with a source-block temperature of 373 K and a desolvation temperature of 623 K. The chromatographic separation was performed using a Vydac Low TFA C4MS column (1 × 150 mm, 5 µm, 300 Å) maintained at 313 K at a flowrate of 200 µl min^{-1}. The mobile phases were (*A*) 0.05% TFA in water and (*B*) 0.0375% TFA in acetonitrile. The proteins were separated using a linear gradient from 10 to 50% *B* over 155 min. The first 20 min of the gradient was diverted to waste, after which the fraction collector began collecting 226 µl fractions. A total of 96 fractions were collected and then dried in a SpeedVac. The proteins in the fractions were reduced, denatured and S-alkylated prior to enzymatic digestion with trypsin (Promega, Inc.) overnight at 310 K.

For MALDI–TOF analysis, the digests were desalted using C18 ZipTips (Millipore Inc.) and eluted directly onto the MALDI sample plate in a saturated solution of α-cyano-4-hydroxycinnamic acid in 0.1% TFA:80% methanol:20% H_2O. A Voyager DE-STR MALDI–TOF Elite mass spectrometer (Applied Biosystems) was operated in reflectron positive-ion mode with delayed extraction and the spectra were initially calibrated externally using Applied Biosystems Calibration Mixture 1. The data were collected in Automatic Control using a 20-point spiral with 50 laser shots per point in accumulate all spectra mode with a mass range from 500 to 4000 Da.

LC-MS/MS analysis was carried out on a Thermo Fisher Scientific LCQ ion-trap mass spectrometer using a data-dependent experiment (DDE). The LC system consisted of an Agilent 1100 Capillary HPLC (5 µl min^{-1} flowrate) with diode-array detector. An Agilent 1100 Micro autosampler injected 8.0 µl aliquots onto a Vydac Low TFA C18MS column (0.32 × 100 mm, 5.0 µm). The mobile phases were (*A*) 0.02% TFA in H_2O and (*B*) 0.02% TFA in acetonitrile.

Each MALDI–TOF data file was processed and a mass list was created and submitted for database searching using the *AutoMS-Fit* package from the Applied Biosystems *Proteomics Solution* 1 (*PS*1) software, using the *Protein Prospector* search engine to perform database searches. Peak Filter was enabled and the mass range of 0–800 Da was ignored. The peptide mass tolerance for the initial search was set to 0.02%. The top 40 most intense peaks were submitted for database searching with the fixed modification of carboxymethylation of cysteines and oxidation of methionine and N-terminus acetylation set to variable. Trypsin was set as the enzyme, with a maximum of four missed cleavages. The Intellical option was enabled with a mass-accuracy cutoff of 20 p.p.m. The database searched was compiled from the NCBI and contained only *D. radiodurans* proteins. The database is not comprehensive and contains many protein sequences that are based only on DNA translation. LC-MS/MS data were searched using *Mascot* (Matrix Sciences) using similar settings and the same database.

Identified proteins in the fractions were compared with the intact mass obtained from the split-flow results for the mass spectrometer. Intact masses were obtained by utilizing the *MaxEnt* deconvolution algorithm from Waters with the resolution set to 1 Da per channel. A uniform Gaussian was used as the Damage model with a width at half-height of 2.8 Da. Minimum intensity ratios of 10% were used and the algorithm was allowed to complete a maximum of ten iterations. The HPLC method and data processing used to identify the proteins was also used when profiling all of the *D. radiodurans* 50S subunit preparations.

2.7. Ribosome crystallization and data collection

Crystallization of subunits was carried out essentially as described previously (Auerbach-Nevo *et al.*, 2005; Harms *et al.*, 2001; Schlunzen *et al.*, 2000) by hanging-drop vapor diffusion in 24-well VDX plates (Hampton Research) at 295 K. The data used for structure determination were collected on the X06SA and X10SA beamlines of the Swiss Light Source (Paul Scherrer Institute) at 100 K.

3. Results

3.1. Cell growth

An early obstacle was obtaining robust growth of the cells. It was found that cells only grew to an optical density (at 600 nm) of about 2 in a standard broth (see §2) containing either tryptone (Difco Inc.) or casein hydrolysate (Oxoid Ltd). Crystallizable 50S subunits were never obtained from these cells, which were misshapen and clumped together (Fig. 1*a*). We set out to improve the growth medium, since the production of large amounts of highly active ribosomes requires robust growth. Substitution with tryptone from Oxoid Ltd (but not other sources) allowed growth to an OD of 15 in shake flasks and dramatically improved the cell morphology (Fig. 1*b*). Fermentor growth to an OD of 3 was then used to produce cells for subunit isolation and all crystallizable subunits were obtained from such cells. The growth medium was supplemented with a trace amount of manganese sulfate, which has been shown to increase growth in certain media (Auerbach-Nevo *et al.*, 2005; He, 2009). However, we did not find that this inclusion altered growth in this particular medium, nor was it subsequently found to affect the production of crystallizable subunits. We also tested the effect of growth pH. The pH of fermentor cultures of *D. radiodurans*

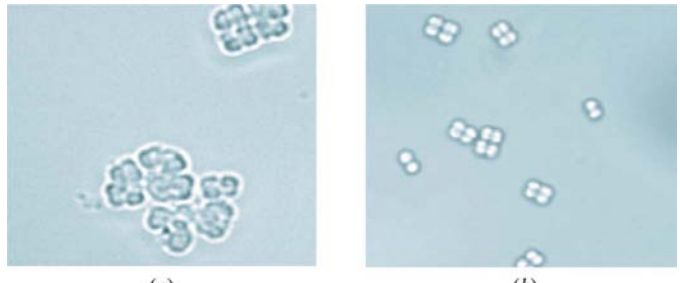

Figure 1
Appearance of *D. radiodurans* cells during growth in medium supplemented with (*a*) Difco tryptone and (*b*) Oxoid tryptone.

growing in the standard medium drops below pH 7.3 during the first 2–3 generations of growth and then increases to 7.4 prior to harvesting. Subunits obtained from cultures whose pH was unregulated, maintained at 7.3 or merely prevented from falling in the initial phase (final pH 7.6) showed no clear differences in crystallization.

3.2. Analytical tests

A central strategy was to assess not only crystallization of the subunits but also their purity, integrity and activity. Contamination by the 30S subunit is a concern when isolating 50S fractions from sucrose density gradients and so was routinely checked by analytical sucrose density gradients. This contamination was kept below a few percent by judicious selection of fractions from the preparative sucrose gradients. Activity was assessed by *in vitro* polyU-directed synthesis of polyphenylalanine.

50S ribosomal subunits from bacteria contain two molecules of ribosomal RNA (rRNA): one small ('5S') rRNA and one larger ('23S') rRNA. These were extracted from the 50S subunits and the integrity of the 23S rRNA was monitored after separation by denaturing PAGE and staining with ethidium bromide.

Ribosomal proteins were extracted from the subunits for analysis. A standard method for the observation of ribosomal proteins is two-dimensional electrophoresis on ribosomal protein gels. Such gels are designed to resolve most ribosomal proteins, but contaminants are usually too large and acidic to enter these gels, so that the staining pattern obtained by electrophoresing pure ribosomes is little different from that obtained from cell lysates (for an example, compare Figs. 1*a* and 1*e* in Maguire *et al.*, 2001). Simple one-dimensional SDS–PAGE does not resolve the ribosomal proteins, but can be used to observe contaminants that are much larger than ribosomal proteins (which are generally <40 kDa; Maguire *et al.*, 2008). However, most 50S subunits prepared by standard centrifugation appear to be pure by this method. We chose LC-MS as our standard method because it detects both large and small contaminants as well as post-translational modification and proteolysis of the ribosomal proteins. It also allows rough comparison of relative contents of individual ribosomal proteins between preparations by comparing the absorbance intensity of their corresponding HPLC peaks. Correlations between crystallization and relative protein content and integrity were sought.

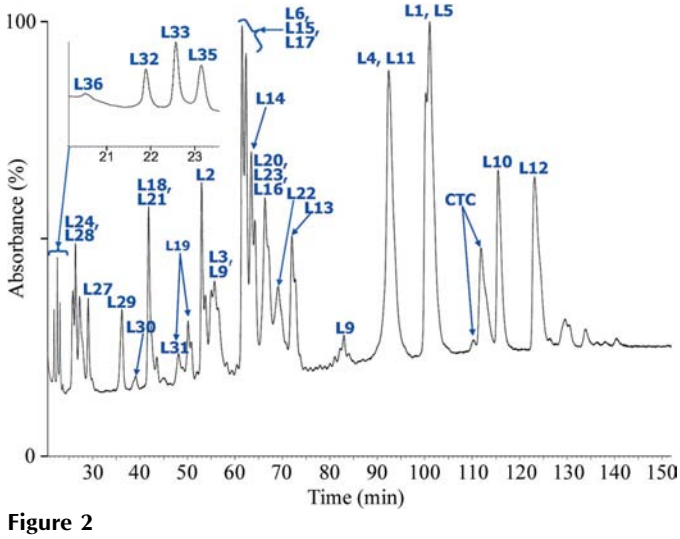

Figure 2
RP-HPLC of 50S ribosomal proteins from *D. radiodurans*. Protein identifications from MS analysis are given on the corresponding absorbance peaks. The inset shows an expanded view of the earliest part of the chromatogram.

3.3. Mass spectrometry of ribosomal proteins

The system was first validated using ribosomal proteins from the *Escherichia coli* 50S subunit, as the ribosomal proteins from this species are known to separate efficiently in RP-HPLC (Cooperman *et al.*, 1988; Kerlavage *et al.*, 1983) and the masses of the intact proteins have been catalogued in several MS studies (Arnold & Reilly, 1999; Chi *et al.*, 2007; Moini & Huang, 2004; Wilcox *et al.*, 2001). All but one (L34) were identified from their intact masses, which matched those published (Arnold & Reilly, 1999; Moini & Huang, 2004; Wilcox *et al.*, 2001). Details of both the LC separation and the observed masses are provided as supplementary material[1] (Supplementary Table 1, Supplementary Fig. 1). No evidence of degradation of the *E. coli* proteins was found in these experiments.

Initial *D. radiodurans* protein identifications were based on the mass predicted by the genome sequence (Supplementary Table 2[1]). The HPLC peaks of *D. radiodurans* 50S subunit proteins were identified by a combination of LC-ESI-MS, LC-ESI-MS/MS and MALDI–TOF MS of tryptic digests. The removal of N-terminal methionines by methionine aminopeptidase followed the expected pattern, seen in other bacteria, of dependence on the adjacent amino acid in the sequence (Flinta *et al.*, 1986). Previously identified errors in the L6, L21, CTC (an L25 homolog) and L33 sequences were confirmed (Harms *et al.*, 2001; PDB entry 1nkw), together with one additional error in protein L13 that was also reported by another group during preparation of this manuscript (Running & Reilly, 2009). The LC separation of the proteins is shown in Fig. 2. The intact masses obtained agreed with those published recently (Running & Reilly, 2009), with the same conclusions drawn concerning post-translational modifications. These modifications are similar to those seen for the *E. coli* homologs, but with additional examples in *D. radiodurans* of L5 (dimethylated) and L22 (acetylated), while unlike in *E. coli* only a single methylation was found for protein L16 and L33 was not modified. Since L7, the mono-acetylated version of L12, was never detected, we conclude that this modification does not occur in *D. radiodurans*, as in some other species (Ilag *et al.*, 2005; Running *et al.*, 2007). Protein L27 mostly lacked its C-terminal aspartate. This aspartate is not a common feature of L27 homologs, but absence of the last

[1] Supplementary material has been deposited in the IUCr electronic archive (Reference: BW5305). Services for accessing this material are described at the back of the journal.

amino acid of L27 has also been reported in *Caulobacter crescentus* (where it is a glutamate; Running *et al.*, 2007).

Progressive C-terminal proteolysis was seen for proteins L19 and CTC; L19 was degraded one residue at a time to remove up to 36 amino acids, while CTC yielded discrete fragments lacking up to 54 amino acids at the C-terminus. Most of the truncated forms of CTC were eluted together from the column; their masses are shown on the deconvoluted mass spectrum in Fig. 3(*a*) together with the position of the cleavages commonly observed in the protein sequence. For L19 the truncated forms were spread over a wide area of the chromatogram, so that no single mass spectrum captured them all. Instead, their spread on the LC chromatogram is indicated in Fig. 3(*b*); the specific cleavages observed in this instance are shown. This proteolysis varied widely in different 50S preparations. Inclusion of a cocktail of protease inhibitors in purification buffers reduced the proteolysis of both proteins (Figs. 3*c* and 3*d*), indicating that it arises during purification. In addition, the levels of proteins L9 and L12 varied in the subunits, but no fragments were detected and the levels were unchanged by protease inhibitors, suggesting that simple dissociation is the cause. Fig. 4 compares the chromatograms obtained from two 50S preparations that differ in their content of L9 and L12 as well as intact L19 and CTC. These variations were monitored to see if they correlated with the behavior of subunits in crystallization. An exception was L19; this was difficult to routinely monitor, but did not show any striking correlation with crystallization and so was not closely followed.

A more general observation was that over time we found that we could differentiate whether a preparation of subunits was sufficiently pure to crystallize or not by monitoring the baseline and any extraneous peaks of the UV trace and the total-ion chromatogram (TIC). An early increase in purity was observed when we improved the growth medium to allow fermentation to a higher density; this may have been a benefit of the increased cellular content of ribosomes during rapid growth relative to potential contaminants.

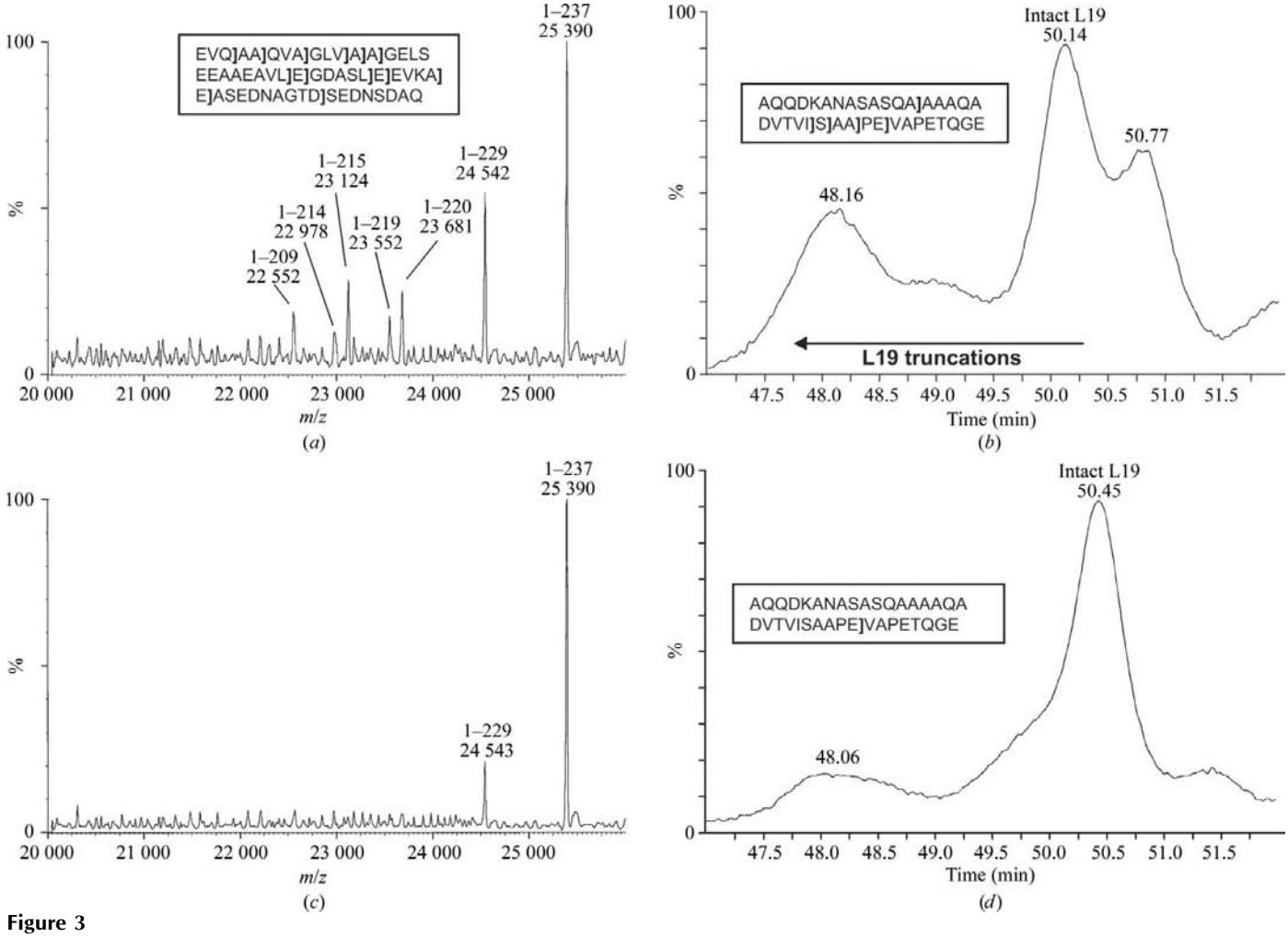

Figure 3

(*a*) Deconvoluted mass spectrum of full-length CTC and its truncation products. 13 sites of cleavage in the last 55 amino acids of the CTC sequence (residues 183–237) observed in different 50S preparations are indicated in the inset by square brackets. C-terminal truncations corresponding to the last seven of these cleavages were detected in this experiment and are indicated above their corresponding *m*/*z* value and peak by their residue numbers (full-length CTC is 1–237). (*c*) The same as (*a*) but from subunits purified in the presence of protease inhibitors. (*b*) LC chromatogram of full-length L19 and its truncation products. Retention times in minutes are indicated on the peaks. Sites of cleavage in the last 36 amino acids of the L19 sequence in this experiment are indicated in the inset by square brackets. (*d*) The same as (*b*) but from subunits purified in the presence of protease inhibitors.

3.4. Purification

Production of ribosome crystals is a fickle process that is notoriously difficult to transfer between different laboratories. Some of our earliest attempts to obtain crystallizable 50S subunits followed the procedure of Auerbach-Nevo *et al.* (2005) in which the polysomes (multiple 70S ribosomes bound to the same molecule of messenger RNA) are spun down from the cell lysate, resuspended in buffer and then centrifuged on a sucrose density gradient made in low-magnesium buffer to dissociate the subunits. Fractions containing the 50S subunits are pooled and the subunits pelleted and resuspended in buffer for storage and subsequent crystallization. Despite many attempts and a close collaboration with considerable support from the original authors (Auerbach-Nevo *et al.*, 2005), we were unable to reproduce their results and only obtained subunits that consistently failed to crystallize (under conditions where subunits they supplied did crystallize). Several minor variations of the protocol were also tested without success. The same failure was encountered when we used a similar supplied protocol that instead isolates the 50S from the remainder of the lysate after polysome removal.

We therefore sought to develop new purification strategies to obtain subunits that crystallize. Our starting point was the isolation of 'tight-couple' ribosomes: a standard procedure used for the isolation of highly active ribosomes from *E. coli* (Spedding, 1990). The association of 30S and 50S subunits as 70S couples is mediated by magnesium ions and tight-couple 70S ribosomes are those that remain associated during centrifugation at a magnesium-ion concentration of 6 m*M*, where 'loose-couple' ribosomes dissociate into subunits (Hapke & Noll, 1976). The two ribosomal subunits interact differently with each other to give tight or loose association and loose couples have a less compact structure (Bonincontro *et al.*, 2001). For *E. coli*, the tight-couple ribosomes are the more active and so are often preferred for functional studies (Noll *et al.*, 1973; Rheinberger *et al.*, 1988). We reasoned that more active subunits might be more likely to crystallize and that separation of the different classes of 50S according to their association (unassociated, loosely associated or tightly associated) would improve homogeneity, since the susceptibility of their protein and rRNA to degradation during isolation may differ between the different classes. Furthermore, although the ribosomal subunits are conformationally flexible, there is some evidence that differences in the conformation and nuclease susceptibility of the 23S rRNA in 50S subunits in loose or tight couples can persist even after 70S dissociation (Burma *et al.*, 1984, 1985).

Details of the procedure are given in §2, but in essence the cell lysate is cleared of unbroken cells and then polysomes by centrifugation. The remaining ribosomes are then pelleted through a layer of 1.1 *M* sucrose to remove protein contaminants. These crude ribosomes were resuspended in buffer and tight-couple 70S were separated from subunits that were

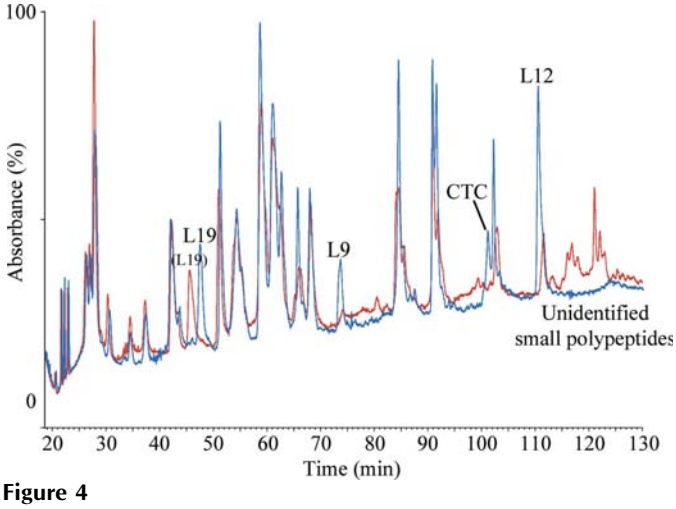

Figure 4
Overlaid RP-HPLC chromatograms of two 50S preparations that differ in their contents of L9, L12 and intact L19 and CTC. A peak corresponding to degraded L19 is labeled in a smaller font in parentheses.

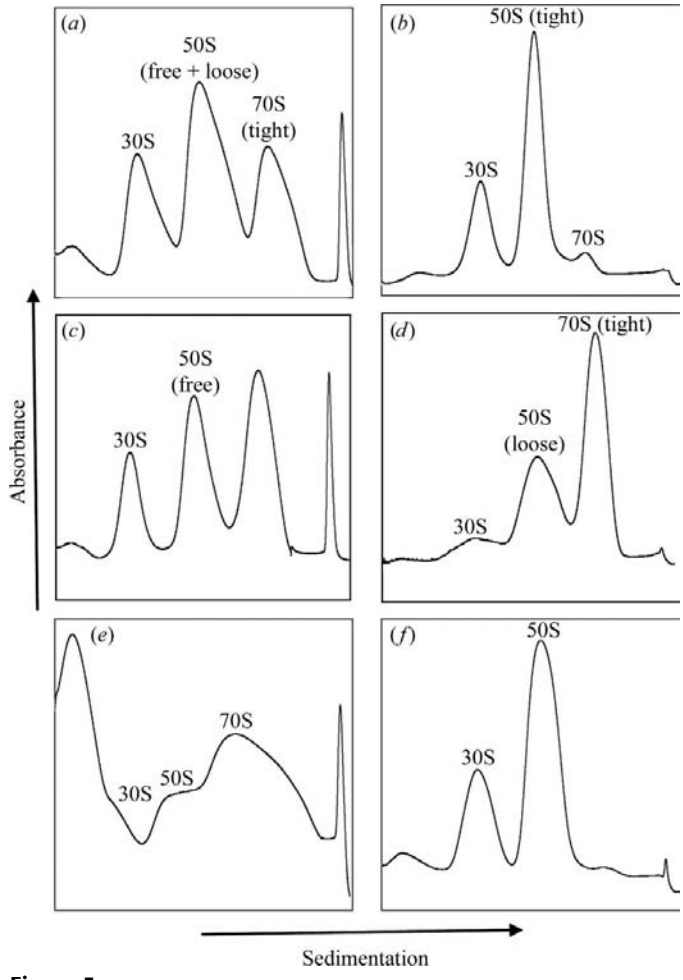

Figure 5
Absorbance traces of ribosomes separated on preparative sucrose density gradients used for 50S subunit purifications. (*a*) Isolation of free/loose-couple-derived 50S at 6 m*M* magnesium-ion concentration. (*b*) Isolation of tight-couple-derived 50S by sedimentation of the 70S fraction from (*a*) on a gradient in 1 m*M* magnesium ion. (*c*) Isolation of free 50S at 30 m*M* magnesium-ion concentration. (*d*) Isolation of loose-couple-derived 50S by sedimentation of the 70S fraction from (*c*) on a gradient in 6 m*M* magnesium ion. (*e*) Direct isolation of 70S at 30 m*M* magnesium-ion concentration. (*f*) Isolation of 50S by sedimentation of the 70S fraction from (*e*) on a gradient in 1 m*M* magnesium ion.

unassociated or loosely associated by centrifugation on a sucrose density gradient in 6 m*M* magnesium ion as shown in Fig. 5(*a*). 50S are then derived from the tight-couple 70S on a second gradient in 1 m*M* magnesium ion to dissociate the subunits as shown in Fig. 5(*b*). The first such preparation yielded crystals from both the tight-couple-derived 50S from the second gradient and the mixed free and loose-couple 50S from the first gradient. Subsequent purifications by the same method gave a 50% success rate. Either both samples from a purification crystallized or both did not, and the quality of the crystals obtained from the tight-couple or free/loose samples was about the same. Although the crystals were small and clustered (Fig. 6*a*) and diffracted poorly (patterns extending only to 10 Å resolution), they provided a starting point for iterative improvement. The low success rate was a handicap, but was also an opportunity to seek correlations of crystallization with other properties such as activity and integrity.

In vitro elongation activity of the preparations in polyU-directed synthesis of polyphenylalanine was compared (Fig. 7). As expected from the literature on *E. coli*, 50S derived from tight couples were more active than those from loose couples. However, no obvious correlation could be found between crystallization (indicated by a plus sign below the plot) and activity. For instance, 50S subunits isolated from polysomes by the original procedure were as active as those isolated from loose-couple 70S monosomes, yet did not crystallize. Subunits from tight couples were more active than those from loose couples but did not crystallize more readily, and the loose- or tight-couple preparations that did crystallize did not show higher or lower activity than those that did not. Our interpretation was that activity was not the limiting factor for crystallization of these different preparations but that other factors must prevent some of them from crystallizing.

A variant of the purification isolated pure unassociated 50S by using 30 m*M* magnesium ion in the first gradient (Fig. 5*c*). Centrifugation of the 70S fraction from this first gradient on a second gradient at 6 m*M* magnesium ion (Fig. 5*d*) yielded pure loose-couple 50S. The latter but not the former crystallized. Thus, crystals could be obtained from 50S that derived from tight or loose couples alone, or loose couple plus free subunits, but not from free subunits alone. Comparison of the rRNA integrity in these preparations (Fig. 8) showed that 50S subunits from pure loose (lane 10) or tight couples (lanes 7 and 8) were the most intact. rRNA from free subunits (lane 9) or the free/loose mixture (lanes 5 and 6) was similarly degraded to that from the original polysome preparations (lanes 3 and 4) that had failed to crystallize. Therefore, as with the activity measurements, a clear correlation with crystallization was not found, but the observations suggested that integrity and activity could be improved by first isolating the 50S as 70S couples on a density gradient. Monitoring of rRNA integrity through the different steps of purification showed that much of the degradation occurred in the early pelleting steps prior to sucrose density gradient centrifugation.

Another inference was that the increased homogeneity from the separation of tight-couple-derived 50S from the free/loose 50S had also benefited crystallization. However, recombining free/loose and tight-couple 50S preparations that were separately crystallizable did not prevent crystallization, suggesting an alternative explanation. We surmised that the use of a high magnesium-ion concentration in the first gradient

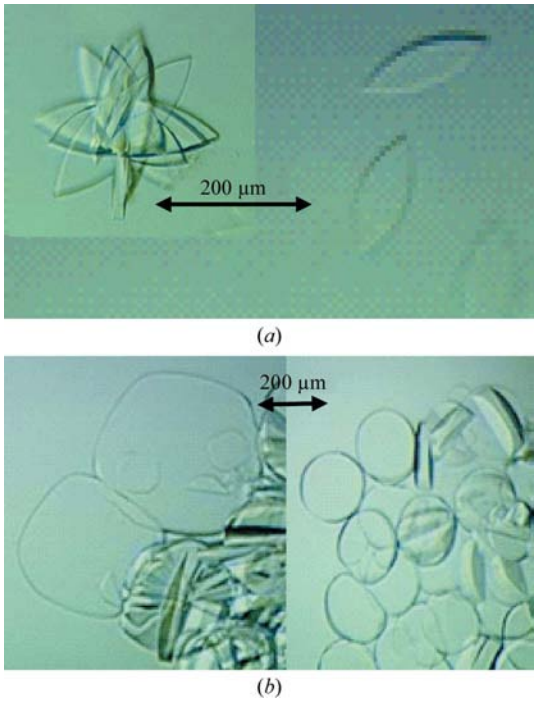

Figure 6
Crystals grown from 50S subunits prepared by different purification methods. (*a*) Crystals typical of free/loose- or tight-couple-derived subunits. These were 100–150 µm in their longest dimension and 25–30 µm thick. (*b*) Crystals typical of subunits isolated by the direct method. These were 200–400 µm in their longest dimension and 50 µm thick. Note the different scales in (*a*) and (*b*).

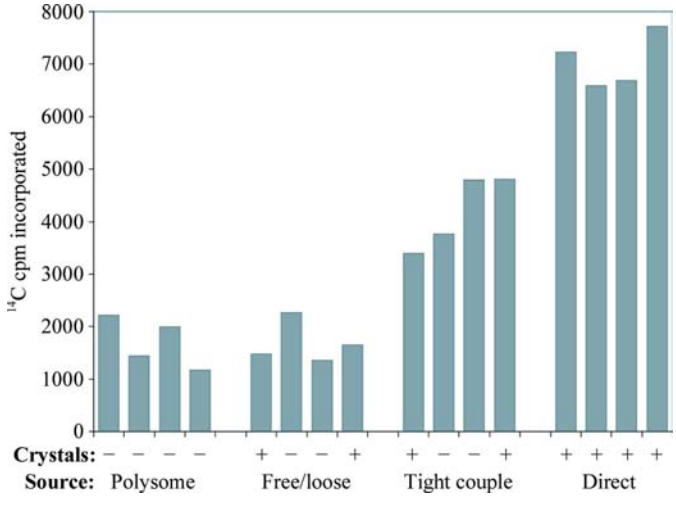

Figure 7
Activity of 50S subunits in polyU-directed synthesis of polyphenylalanine *in vitro*. Typical examples are given for 50S purified from polysomes, mixed free/loose-couple-derived 50S, tight-couple-derived 50S or 50S purified by the direct-isolation protocol. The success or failure of each preparation to crystallize is indicated below the plot by a '+' or a '−', respectively.

(6 m*M* as opposed to 1 m*M* in the unsuccessful early protocols) had somehow conferred an advantage.

Comparisons of the contents of ribosomal proteins L9 and L12 and the integrity of the CTC protein are shown for some representative samples in Fig. 9. It can be seen that the contents of L9, L12 and intact CTC are very low for both loose- and tight-couple-derived 50S but that their levels do not appear to differentiate between loose- and tight-couple 50S that do or do not crystallize. The low levels of the proteins in the loose- and tight-couple 50S is largely the consequence of a dialysis step employed prior to gradient centrifugation. This was a remnant from an earlier supplied protocol and was not present in the polysome protocol that we obtained, so that the 50S we had derived from polysomes had much higher levels of the proteins. We found that dialysis not only promoted loss of L9 and L12, but also degradation of L19 and CTC.

In theory, degradation of CTC might remove disordered regions that could impede crystallization, and the removal of flexible protein appendages such as L12 and L9 could also be beneficial. However, we felt that a high level of integrity was worth pursuing as the best guarantee of homogeneity, especially since the published crystallographic structure contained L9 and at least some of the L12 copies (Harms *et al.*, 2001). The accumulating evidence suggested that integrity could be improved by isolating the 70S directly from the lysate on a sucrose gradient made in high-magnesium buffer and without prior steps (Fig. 5*e*), and that this might benefit crystallization. The 50S subunits would then be isolated on a second sucrose gradient in 1 m*M* magnesium ion (Fig. 5*f*).

This prediction was confirmed as this 'direct' isolation invariably gave subunits that showed robust crystallization and gave crystals that initially gave diffraction patterns that extended to 3.5 Å resolution. Further improvement in crystallization was obtained by using ultrafiltration rather than pelleting to recover the 70S from gradient fractions. This gave crystals that were large enough to obtain a whole data set without tedious merging of data sets from multiple crystals. Typical crystal morphology is shown in Fig. 6(*b*). The use of a microfocused beamline with these larger crystals allowed us to extend diffraction patterns to 2.9 Å resolution for apo crystals into which antibiotics had successfully been soaked. Fig. 10 shows a typical diffraction pattern.

As expected, protein integrity was improved (Fig. 9) with high levels of the three proteins, although this was not the case for all proteins in all preparations. Activity was also greatly improved (Fig. 7), but the integrity of the rRNA was not as high as for the tight-couple-derived and pure loose-couple-derived 50S (Fig. 8, lanes 11 and 12). Several factors may be

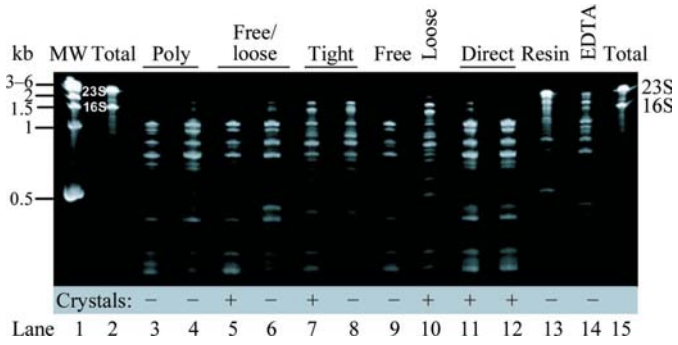

Figure 8
Ethidium bromide-stained rRNA isolated from different 50S preparations and resolved by denaturing PAGE. Lane 1, molecular-weight markers. Lanes 2 and 15, intact 16S and 23S rRNA. Lanes 3 and 4, rRNA from 50S isolated from polysomes. Lanes 5 and 6, rRNA isolated from mixed free/loose-couple 50S. Lanes 7 and 8, rRNA from 50S isolated from tight couples. Lane 9, rRNA from free 50S. Lane 10, rRNA from 50S isolated from pure loose couples. Lanes 11 and 12, rRNA from direct-isolation 50S. Lane 13, rRNA from direct isolation preceded by cysteine-Sulfolink chromatography. Lane 14, rRNA from direct isolation in the presence of EDTA. The success or failure of each preparation to crystallize is indicated below the plot by a '+' or a '−', respectively.

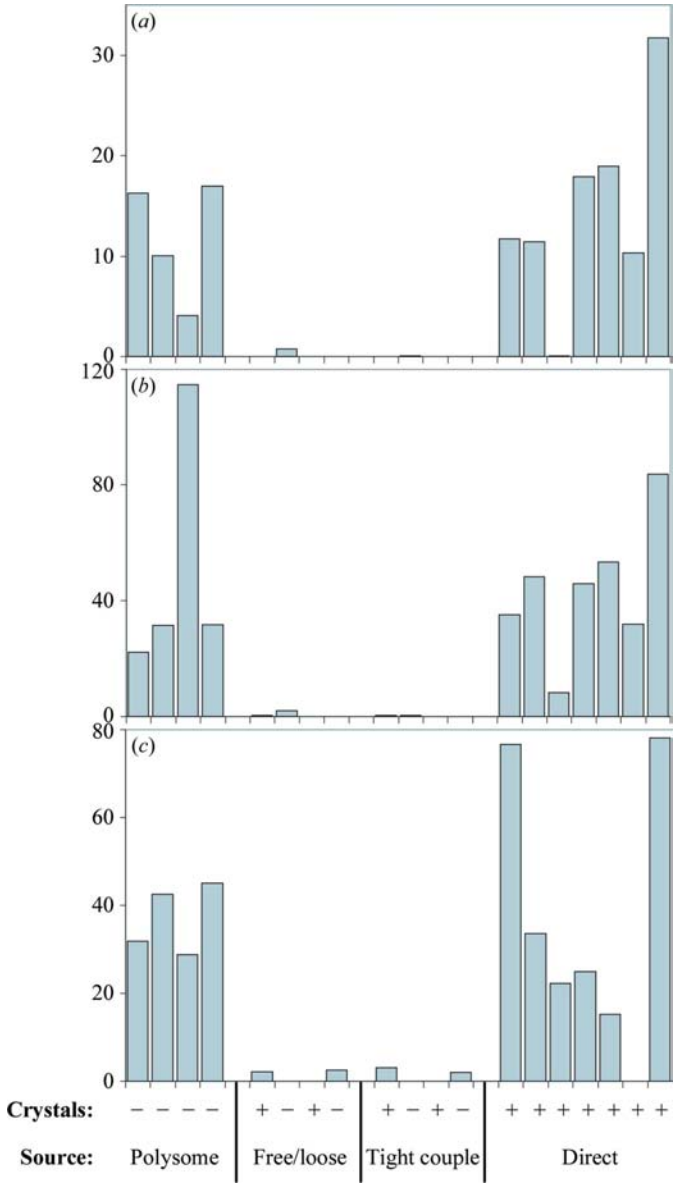

Figure 9
Variable proteins detected by LC-MS in 50S preparations purified by different methods as indicated below the plots. (*a*) Relative levels of protein L9. (*b*) Relative levels of protein L12. (*c*) Percentage of total CTC protein detected intact. The success or failure of each preparation to crystallize is indicated below the plot by a '+' or a '−', respectively.

working in concert so that subunits prepared in this way form larger better diffracting crystals more readily than the previous loose/tight isolation.

In 20 purifications, our standard direct-isolation protocol never failed to produce subunits that crystallized, so that many variants could now be tested to determine the critical features of the protocol and find improvements. One strategy to improve homogeneity was to process up to four separate pools from different parts of the 50S peak on the second sucrose gradient, rather than pooling them together. Another was to make the second gradient in 6 m*M* magnesium ion to isolate 50S only from loose couples. A third was to make the first gradient in 6 m*M* magnesium ion to allow isolation of 50S only from tight couples on the second gradient (at 1 m*M* Mg^{2+}). None of these improved crystal quality.

Polysomes could be removed before the first sucrose gradient; this reduced yields but did not affect crystallization. However, reintroduction of the step that pelleted the ribosomes through a cushion of 1.1 *M* sucrose and then resuspended them prior to the first gradient abolished crystallization. This step had been necessary for free/loose 50S preparations to ensure sufficient purity for crystallization, but is replaced in the direct isolation by the first gradient, which avoids pelleting the 70S. The preparative-scale purification of ribosomes directly on sucrose-density gradients represents something of a break with tradition, as differential pelleting spins prior to density-gradient centrifugation have long been standard practice. Since quality appeared to be improved by avoiding pelleting and resuspension of the ribosomes, we were encouraged in parallel efforts, discussed later, to develop purifications based on chromatography rather than centrifugation.

Although standard SDS–PAGE of ribosomal proteins showed little difference between most preparations, about half of the 50S preparations made by direct isolation did show a prominent contaminant on one-dimensional SDS–PAGE (indicated by an arrow in Fig. 11, lanes 12 and 14). This could be removed by pelleting the purified subunits through a 1.1 *M* sucrose cushion (Fig. 11, lane 13) without affecting crystallization. MALDI-MS of an in-gel tryptic digest of this band identified the protein as the E1 component of the pyruvate dehydrogenase complex. It presumably does not interfere with crystallization as it is not a ribosome ligand, but rather part of a high-molecular-weight complex that co-sediments with the 50S subunit on sucrose density gradients (Jiang *et al.*, 2006). For 50S prepared by direct isolation, the first gradient is apparently sufficient to remove the important contaminants. Reintroduction of the pelleting through 1.1 *M* sucrose prevents subsequent crystallization, unless it is performed only at the end of the protocol after the 50S subunits have been isolated. The operative factor seems to be to isolate 70S quickly and gently; subsequent steps can include pelleting, although the improvement seen with ultrafiltration suggests that avoiding such spins for the 70S is beneficial. Faster isolation could be achieved by halving the sucrose concentrations in the first sucrose gradient to reduce spin times from 16.5 to 5.5 h, but this did not influence crystallization. Once isolated by our standard method, the 70S could be flash-frozen and processed later on the second sucrose gradient without loss of subsequent crystal quality.

Further clues come from the production of subunits by chromatography. We have developed a novel method to purify highly intact ribosomes by chromatography on cysteine-Sulfolink resin (Maguire *et al.*, 2008). The pyruvate dehydrogenase complex protein could also be removed from 50S subunits by this chromatography (Fig. 11, lane 15) without compromising crystallization. However, if ribosomes were purified first on this resin and 50S was then isolated by our standard method on sucrose density gradients (either a single gradient in 1 m*M* magnesium ion or one in 30 m*M* followed by another in 1 m*M*) they failed to crystallize.

The chromatography itself does not prevent the crystallization of otherwise crystallizable subunits. Other forms of chromatography have also been successfully employed to produce crystallizable ribosomes from *T. thermophilus* (Petry *et al.*, 2005; Korostelev *et al.*, 2006; Clemons *et al.*, 2001). However, ribosomes isolated from cell lysates of *D. radiodurans* by cysteine-Sulfolink chromatography have unusually intact rRNA (Maguire *et al.*, 2008). This was the case for the subunits purified first on cysteine-

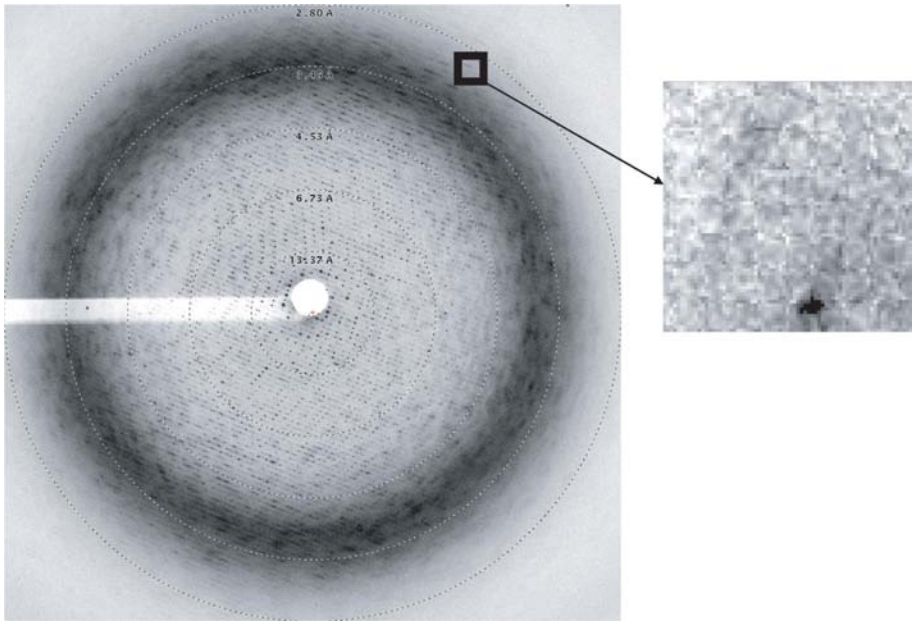

Figure 10
Typical diffraction of a crystal soaked with an antibiotic candidate obtained using *D. radiodurans* 50S ribosomal subunits purified by the new 'direct' isolation method. The inset shows diffraction spots extending to 2.9 Å resolution. Data were collected on beamline X10SA of the SLS.

Sulfolink and then by centrifugation (Fig. 8, lane 13), suggesting that fully intact rRNA may actually hinder crystallization of the *D. radiodurans* 50S subunit.

Additional evidence was provided by purification in buffers supplemented with low concentrations of EDTA (§2). EDTA inhibited degradation of the ribosomal RNA (Fig. 8, lane 14) and the resulting 50S did not crystallize. However, if subunits that had already been isolated by the standard method were incubated with EDTA, pelleted and resuspended in buffer without EDTA, their ability to crystallize was unimpaired. This suggests that it is not the exposure to EDTA itself that is the problem (for instance, by removal of a critical trace cation), but rather its effect on rRNA degradation during early purification steps. However, attempts to prove the corollary and render the subunits crystallizable by controlled nicking of the intact rRNA (using immobilized RNase T1) were unsuccessful.

4. Discussion

Mass spectrometry formed an important part of our assessment of 50S purification for crystallization. Detailed information was not previously available on the integrity and purity of ribosomal proteins in crystallizable subunits. Proteins L9, L12, L19 and CTC were found to be a source of variability through their dissociation or degradation. The location of these proteins on the 50S subunit of *D. radiodurans* is shown in Fig. 12. In *E. coli* the protein L7/L12 stalk is composed of two copies each of L7 and L12 arranged as a tetramer (Pettersson *et al.*, 1976). This flexible appendage is not resolved in the crystallographic structure, but its approximate location is indicated in the figure. The L7/L12 stalk is loosely bound to the *E. coli* 50S and can be dissociated by salt-washing of ribosomes during purification (Gnirke *et al.*, 1989) or by incubation in 50% ethanol (Tokimatsu *et al.*, 1981). Although we did not salt-wash the ribosomes, possible dissociation of L12 from the 50S of *D. radiodurans* was thus anticipated.

In contrast, dissociation of protein L9 was not expected. In *E. coli*, L9 binds independently to 23S rRNA and is one of the more firmly bound proteins, requiring relatively high salt concentrations (>1 *M* LiCl) to strip it from the ribosome (Homann & Nierhaus, 1971). Protein L9 is comprised of an N-terminal and a C-terminal globular domain connected by an α-helix to give a dumbbell shape (Hoffman *et al.*, 1994). X-ray crystallographic structures of the 50S subunit in 70S couples from *E. coli* (Schuwirth *et al.*, 2005) and *T. thermophilus* (Selmer *et al.*, 2006) show the N-terminal domain anchored on the subunit with the C-terminal domain extending away from

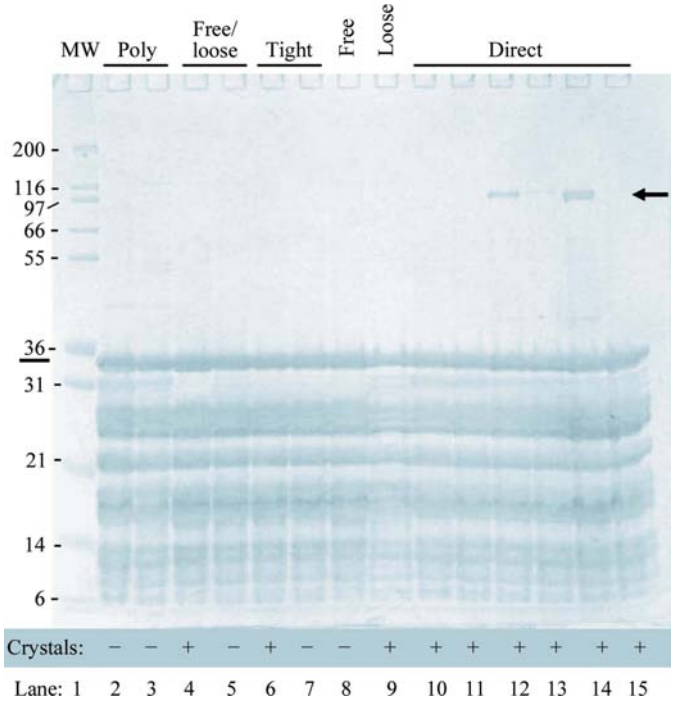

Figure 11
SDS–PAGE of ribosomal proteins (stained with Coomassie Blue) isolated from 50S preparations purified by different methods as indicated above the plots. Lane 1, molecular-weight markers. Lanes 2 and 3, 50S isolated from polysomes. Lanes 4 and 5, mixed free/loose-couple-derived 50S. Lanes 6 and 7, 50S from tight couples. Lane 8, free 50S. Lane 9, 50S from loose couples. Lanes 10–15, 50S from direct isolation. Lane 13 contains proteins from the subunits of lane 12 after sedimentation through 1.1 *M* sucrose and lane 15 contains proteins from the subunits of lane 14 after further purification on cysteine-Sulfolink resin. A prominent contaminant in lanes 12 and 14 is indicated by an arrow. The success or failure of each preparation to crystallize is indicated below the plot by a '+' or a '−', respectively.

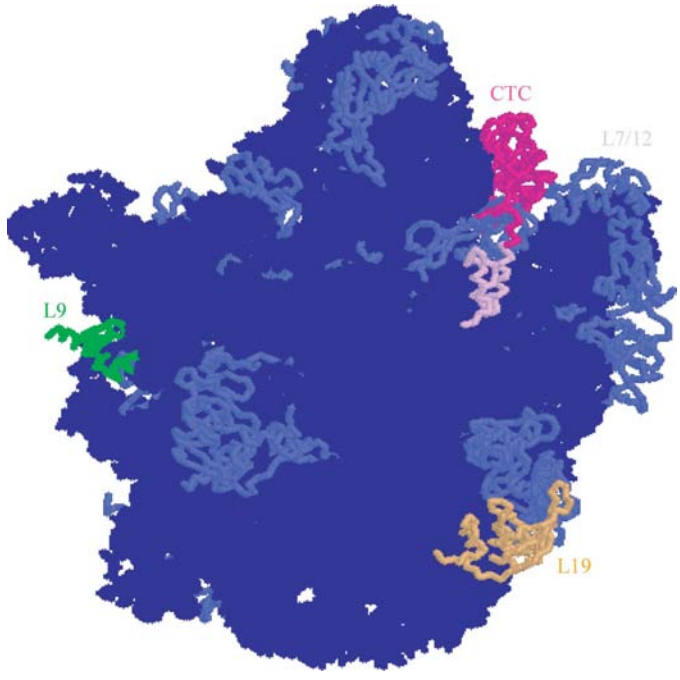

Figure 12
Locations of the variable proteins in the 50S subunit of *D. radiodurans*. RNA is rendered in dark blue. Protein L19 (residues 2–126) is colored orange; the variably truncated residues (130–166) are not seen. Protein CTC is colored magenta with variably removed residues (184–223) in light pink; residues 224–237 are absent. The L12 stalk is absent from the structure, but its location is indicated. Residues 1–52 of the dissociable protein L9 are shown in green. Other proteins are rendered in light blue. *Protein Explorer* (http://www.proteinexplorer.org) and PDB entry 1nkw (Harms *et al.*, 2001) were used to model the subunit.

the subunit; a similar arrangement is suggested by the incomplete L9 density in the *D. radiodurans* 50S structure, in which only the N-terminal domain and part of the connecting helix are visible (Fig. 12). L9 may be somewhat mobile, as cross-linking and chemical probing of *E. coli* 50S subunits in solution suggest that the C-terminus can also be found on the surface of the subunit (Lieberman *et al.*, 2000; Osswald *et al.*, 1990). Surprisingly, there is also evidence that it may be the only ribosomal protein capable of exchange between 50S subunits *in vivo* (Robertson *et al.*, 1978; Subramanian & Van Duin, 1977).

The CTC (catabolite-controlled) protein of *D. radiodurans* is an interesting protein that is comprised of three domains, each with a specific function. The N-terminal domain (domain I) is homologous to the 5S rRNA-binding protein L25 of *E. coli*, while domain II is known as the CTC domain. CTC was first identified in *Bacillus subtilis* as a general stress-response protein which is incorporated into the ribosome during the stress reponse, but it is a permanent component in the ribosomes of other species (Schmalisch *et al.*, 2002). The third domain of *D. radiodurans* CTC has no counterpart in other species (Harms *et al.*, 2001). It reaches down into the A-site, but changes conformation to move out of the way upon binding of a mimic of the aminoacyl-tRNA (Bashan *et al.*, 2003), leading to the suggestion that it may influence tRNA binding in times of stress (Zarivach *et al.*, 2004). This part of the molecule is prone to proteolysis in our experiments and only part of it is resolved in the *D. radiodurans* 50S subunit crystal structure, suggesting mobility and/or proteolysis.

The portion of protein L19 that is prone to proteolysis has an unusual composition that is 43% alanine or glutamine. This portion is absent in the *D. radiodurans* crystal structure, while the homologous sequence in the *T. thermophilus* 70S crystal structure extends towards the 30S subunit in a helical conformation. Protein L19 is involved in intersubunit contacts in the 70S ribosome and has been found to be protected from tryptic digestion by subunit association (Hamburg *et al.*, 2009).

Analytical techniques helped to guide the improvement of our subunit purification to yield diffraction on a par with that from other methods, with robust crystallization from all 20 such preparations made over several years. However, despite this systematic progress the exact parameters that confer the ability to crystallize remain elusive. The improved activity and overall protein integrity of the 50S might contribute to the improved reliability of crystallization, yet 50S subunits from a collaborator that form crystals with similar diffraction properties had low content and integrity for these proteins, ruling out protein integrity as a key factor. Furthermore, we have provided evidence that improvement of activity over a minimal level does not necessarily correlate with crystallization and the most active preparations are those with the most intact 23S rRNA, which do not crystallize. Some nicking of the 23S rRNA of this species may therefore be required. The answer could lie in some stable conformational difference. Given the inherent flexibility of the 50S subunit, it may not be possible to fix conformational differences in the absence of ligands, but the balance between its different conformations could be tipped by more subtle changes such as particular rRNA cleavages.

Comparison of alternative purification methods and mixing and matching of purification steps from different protocols has been a fruitful way to eliminate some of the variables under consideration. In a second long-term strategy, pursued in parallel with centrifugation efforts, we developed a tag-based purification of *D. radiodurans* 50S (Simons *et al.*, 2009). In essence, the method utilizes a tag to both purify the 50S subunits and to simultaneously sort them according to their association status: unassociated, loosely or tightly associated. None of these have so far yielded crystals despite extensive robotic screening of crystallization conditions, but in this case gross differences in rRNA integrity cannot be invoked, as the 23S appears similar to that from crystallizable 50S obtained by centrifugation. The buffers used are the same as those for centrifugation except that a lower concentration of magnesium ions (0.25 m*M*) is required for 70S dissociation than during centrifugation (1 m*M*) because the high hydrodynamic pressures generated during centrifugation assist dissociation (Pande & Wishnia, 1986). Since magnesium is an important component of the ribosome (Klein *et al.*, 2004), we verified that incubation in this low concentration of magnesium ions did not affect the crystallization of subunits prepared using our standard method.

Alternatively, the elusive factor may be a smaller entity than the macromolecules we have already monitored. It is tempting to speculate that there is something about the unusual physiology of *D. radiodurans* that influences the crystallization of its ribosomes. A high cellular concentration of manganese is thought to contribute to the resistance of *D. radiodurans* to radiation and desiccation by limiting protein oxidation (Fredrickson *et al.*, 2008) and so might affect subunit quality. Although we did not need to supplement the growth medium with manganese to obtain crystals, the cells would still concentrate it from the rich broth they are grown in. However, the fact that washing 50S subunits with EDTA (in the presence of magnesium) did not affect their subsequent crystallization makes a critical role for manganese less likely. Ribosomes from *D. radiodurans* have been shown to contain more magnesium ions than those from *E. coli* (Suessmuth & Widmann, 1979). Given the importance of this ion to ribosome function and integrity (Klein *et al.*, 2004), this might result in greater order, enhancing crystallization. Another feature of *D. radiodurans* is its unusual polyamine content (Gvozdiak *et al.*, 1998). Polyamines are critical to ribosome structure and activity (Xaplanteri *et al.*, 2005) and common ones such as spermidine are often included in crystallization buffers (Yonath *et al.*, 1982); it could be that some of the rarer ones seen in *D. radiodurans* favor crystallization. Such a component would have to remain bound to the subunits during chromatography on cysteine-Sulfolink resin, but this is likely given the low salt concentration (0.3 *M* NH_4Cl) that is used briefly in this chromatography compared with that (0.5 *M* NH_4Cl) required to strip polyamines from ribosomes during successive overnight incubations (Kalpaxis *et al.*, 1986).

Determining the precise factors that potentiate ribosome crystallization remains a significant challenge, but we have greatly narrowed the search while also providing a procedure for the routine production of high-quality *D. radiodurans* 50S subunit crystals that is robust enough to drive industrial structure-based drug design.

References

Arnold, R. J. & Reilly, J. P. (1999). *Anal. Biochem.* **269**, 105–112.

Auerbach-Nevo, T., Zarivach, R., Peretz, M. & Yonath, A. (2005). *Acta Cryst.* D**61**, 713–719.

Bashan, A., Agmon, I., Zarivach, R., Schluenzen, F., Harms, J., Berisio, R., Bartels, H., Franceschi, F., Auerbach, T., Hansen, H. A. S., Kossoy, E., Kessler, M. & Yonath, A. (2003). *Mol. Cell*, **11**, 91–102.

Bohlen, K. von, Makowski, I., Hansen, H. A., Bartels, H., Berkovitch-Yellin, Z., Zaytzev-Bashan, A., Meyer, S., Paulke, C., Franceschi, F. & Yonath, A. (1991). *J. Mol. Biol.* **222**, 11–15.

Bonincontro, A., Nierhaus, K. H., Onori, G. & Risuleo, G. (2001). *FEBS Lett.* **490**, 93–96.

Burma, D. P., Srivastava, A. K., Srivastava, S. & Dash, D. (1985). *J. Biol. Chem.* **260**, 10517–10525.

Burma, D. P., Srivastava, A. K., Srivastava, S., Tewari, D. S., Dash, D. & Sengupta, S. K. (1984). *Biochem. Biophys. Res. Commun.* **124**, 970–978.

Chi, A., Bai, D. L., Geer, L. Y., Shabanowitz, J. & Hunt, D. F. (2007). *Int. J. Mass Spectrom.* **259**, 197–203.

Clemons, W. M. Jr, Brodersen, D. E., McCutcheon, J. P., May, J. L. C., Carter, A. P., Morgan-Warren, R. J., Wimberly, B. T. & Ramakrishnan, V. (2001). *J. Mol. Biol.* **310**, 827–843.

Cooperman, B. S., Weitzmann, C. J. & Buck, M. A. (1988). *Methods Enzymol.* **164**, 523–532.

Flinta, C., Persson, B., Joernvall, H. & Von Heijne, G. (1986). *Eur. J. Biochem.* **154**, 193–196.

Fredrickson, J. K., Li, S. W., Gaidamakova, E. K., Matrosova, V. Y., Zhai, M., Sulloway, H. M., Scholten, J. C., Brown, M. G., Balkwill, D. L. & Daly, M. J. (2008). *ISME J.* **2**, 393–403.

Gluehmann, M., Zarivach, R., Bashan, A., Harms, J., Schluenzen, F., Bartels, H., Agmon, I., Rosenblum, G., Pioletti, M., Auerbach, T., Avila, H., Hansen, H. A. S., Franceschi, F. & Yonath, A. (2001). *Methods*, **25**, 292–302.

Gnirke, A., Geigenmueller, U., Rheinberger, H. J. & Nierhaus, K. H. (1989). *J. Biol. Chem.* **264**, 7291–7301.

Gvozdiak, O. R., Schumann, P., Griepenburg, U. & Auling, G. (1998). *Syst. Appl. Microbiol.* **21**, 279–284.

Hamburg, D.-M., Suh, M.-J. & Limbach, P. A. (2009). *Biopolymers*, **91**, 410–422.

Hapke, B. & Noll, H. (1976). *J. Mol. Biol.* **105**, 97–109.

Harms, J., Schluenzen, F., Zarivach, R., Bashan, A., Gat, S., Agmon, I., Bartels, H., Franceschi, F. & Yonath, A. (2001). *Cell*, **107**, 679–688.

Hartman, H., Favaretto, P. & Smith, T. F. (2006). *Archaea*, **2**, 1–9.

He, Y. (2009). *J. Ind. Microbiol. Biotechnol.* **36**, 539–546.

Hoffman, D. W., Davies, C., Gerchman, S. E., Kycia, J. H., Porter, S. J., White, S. W. & Ramakrishnan, V. (1994). *EMBO J.* **13**, 205–212.

Homann, H. E. & Nierhaus, K. H. (1971). *Eur. J. Biochem.* **20**, 249–257.

Ilag, L. L., Videler, H., McKay, A. R., Sobott, F., Fucini, P., Nierhaus, K. H. & Robinson, C. V. (2005). *Proc. Natl Acad. Sci. USA*, **102**, 8192–8197.

Jiang, M., Datta, K., Walker, A., Strahler, J., Bagamasbad, P., Andrews, P. C. & Maddock, J. R. (2006). *J. Bacteriol.* **188**, 6757–6770.

Kalpaxis, D. L., Theocharis, D. A. & Coutsogeorgopoulos, C. (1986). *Eur. J. Biochem.* **154**, 267–271.

Kerlavage, A. R., Hasan, T. & Cooperman, B. S. (1983). *J. Biol. Chem.* **258**, 6313–6318.

Klein, D. J., Moore, P. B. & Steitz, T. A. (2004). *RNA*, **10**, 1366–1379.

Korostelev, A., Trakhanov, S., Laurberg, M. & Noller, H. F. (2006). *Cell*, **126**, 1065–1077.

Lieberman, K. R., Firpo, M. A., Herr, A. J., Nguyenle, T., Atkins, J. F., Gesteland, R. F. & Noller, H. F. (2000). *J. Mol. Biol.* **297**, 1129–1143.

Maguire, B. A., Manuilov, A. V. & Zimmermann, R. A. (2001). *J. Bacteriol.* **183**, 6565–6572.

Maguire, B. A., Wondrack, L. M., Contillo, L. G. & Xu, Z. (2008). *RNA*, **14**, 188–195.

Moini, M. & Huang, H. (2004). *Electrophoresis*, **25**, 1981–1987.

Noll, M., Hapke, B. & Noll, H. (1973). *J. Mol. Biol.* **80**, 519–529.

Osswald, M., Greuer, B. & Brimacombe, R. (1990). *Nucleic Acids Res.* **18**, 6755–6760.

Pande, C. & Wishnia, A. (1986). *J. Biol. Chem.* **261**, 6272–6278.

Petry, S., Brodersen, D. E., Murphy, F. V. IV, Dunham, C. M., Selmer, M., Tarry, M. J., Kelley, A. C. & Ramakrishnan, V. (2005). *Cell*, **123**, 1255–1266.

Pettersson, I., Hardy, S. J. S. & Liljas, A. (1976). *FEBS Lett.* **64**, 135–138.

Rheinberger, H. J., Geigenmueller, U., Wedde, M. & Nierhaus, K. H. (1988). *Methods Enzymol.* **164**, 658–670.

Robertson, W. R., Dowsett, S. J. & Hardy, S. J. S. (1978). *Mol. Gen. Genet.* **157**, 205–214.

Running, W. E., Ravipaty, S., Karty, J. A. & Reilly, J. P. (2007). *J. Proteome Res.* **6**, 337–347.

Running, W. E. & Reilly, J. P. (2009). *J. Proteome Res.* **8**, 1228–1246.

Schluenzen, F., Tocilj, A., Zarivach, R., Harms, J., Gluehmann, M., Janell, D., Bashan, A., Bartels, H., Agmon, I., Franceschi, F. & Yonath, A. (2000). *Cell*, **102**, 615–623.

Schmalisch, M., Langbein, I. & Stulke, J. (2002). *J. Mol. Microbiol. Biotechnol.* **4**, 495–501.

Schuwirth, B. S., Borovinskaya, M. A., Hau, C. W., Zhang, W., Vila-Sanjurjo, A., Holton, J. M. & Cate, J. H. D. (2005). *Science*, **310**, 827–834.

Selmer, M., Dunham, C. M., Murphy, F. V. IV, Weixlbaumer, A., Petry, S., Kelley, A. C., Weir, J. R. & Ramakrishnan, V. (2006). *Science*, **313**, 1935–1942.

Simons, S. P., McLellan, T. J., Aeed, P. A., Zaniewski, R. P., Desbonnet, C. R., Wondrack, L. M., Marr, E. S., Subashi, T. A., Dougherty, T. J., Xu, Z., Wang, I.-K., LeMotte, P. K. & Maguire, B. A. (2009). *Anal. Biochem.* **395**, 77–85.

Spedding, G. (1990). Editor. *Ribosomes and Protein Synthesis*, pp. 1–29. Oxford University Press.

Subramanian, A. R. & Van Duin, J. (1977). *Mol. Gen. Genet.* **158**, 1–9.

Suessmuth, R. & Widmann, A. (1979). *Z. Naturforsch. C*, **34**, 565–569.

Tokimatsu, H., Strycharz, W. A. & Dahlberg, A. E. (1981). *J. Mol. Biol.* **152**, 397–412.

Wilcox, S. K., Cavey, G. S. & Pearson, J. D. (2001). *Antimicrob. Agents Chemother.* **45**, 3046–3055.

Wilson, D. N., Harms, J. M., Nierhaus, K. H., Schluenzen, F. & Fucini, P. (2005). *Biol. Chem.* **386**, 1239–1252.

Wimberly, B. T., Brodersen, D. E., Clemons, W. M. Jr, Morgan-Warren, R. J., Carter, A. P., Vonrhein, C., Hartsch, T. & Ramakrishnan, V. (2000). *Nature (London)*, **407**, 327–339.

Xaplanteri, M. A., Petropoulos, A. D., Dinos, G. P. & Kalpaxis, D. L. (2005). *Nucleic Acids Res.* **33**, 2792–2805.

Yonath, A. (2002). *Curr. Protein Pept. Sci.* **3**, 67–78.

Yonath, A., Müssig, J. & Wittmann, H. G. (1982). *J. Cell. Biochem.* **19**, 145–155.

Yonath, A. E., Muessig, J., Tesche, B., Lorenz, S., Erdmann, V. A. & Wittmann, H. G. (1980). *Biochem. Int.* **1**, 428–435.

Zarivach, R. *et al.* (2004). *J. Phys. Org. Chem.* **17**, 901–912.